THE ANNALS OF "DUNĂREA DE JOS" UNIVERSITY OF GALAȚI
FASCICLE V, TECHNOLOGIES IN MACHINE BUILDING,
ISSN 2668-4829 (PRINT) 2668-4888 (ONLINE)
https://doi.org/10.35219/tmb.2024.1.01

ROUGHNESS, AMPLITUDE DISTRIBUTION AND BEARING AREA CURVE DURING CNC MACHINING OF Al7SiMg

Nicușor BAROIU[1,2], Virgil Gabriel TEODOR[1,2], Mariana ILIE[1], Georgiana-Alexandra MOROȘANU[2], Răzvan Sebastian CRĂCIUN[1,2]

[1] Department of Manufacturing Engineering, "Dunărea de Jos" University of Galați, România
[2] Research Center in Manufacturing Engineering Technology (ITCM), "Dunărea de Jos" University of Galați, România

email: Razvan.Craciun@ugal.ro

ABSTRACT

The paper analyzes the roughness of surfaces obtained by CNC machining on a HAAS VF-1 center using Al7SiMg type material. The study presents general notions related to microgeometrical precision, roughness parameters, and their impact on the performance of machine parts, such as wear resistance, corrosion, adjustments, and fatigue limit. In the experiments, three surfaces of a part called a hydraulic distributor were machined using a drill, cylindrical-frontal end mill, and frontal end mill tools. Roughness was measured on various surfaces using the Surtronic SJ-210 Mitutoyo equipment, which provides precise results in numerical and graphical form. The findings include roughness values and graphs for each analyzed surface, complemented by graphical representations such as histograms and distribution function curves. The study also highlights the interaction between CNC machining parameters and surface quality, providing useful information for optimizing the machining processes of aluminum alloy materials.

KEYWORDS: roughness, CNC machining, drilling, milling, Surtronic SJ-210 Mitutoyo

1. INTRODUCTION

Devices and machines are built from component parts, subassemblies and assemblies. The machining process involves various devices, pieces of equipment, machinery etc., which are not always perfect, resulting in parts that may deviate from their intended microgeometry, dimensions or geometric shapes.

The processed part will have deviations from the geometrical shape, dimensions etc., due to errors in the processing tools and working methods [1].

Processing errors represent the difference between the part as shown in the drawing and the processed one. Processing precision is represented by the similarity degree between the execution drawing and the processed part. The aspects of the similarity include: geometric shape precision; positional precision; and dimensional precision [1,2].

The causes of processing errors are [1,3]:

- tool wear: occurs due to friction between the processed part and the tool surface; during the machining process, wear alters the geometric shape and dimensions of the parts;
- vibrations of the technological system: can arise during the cutting process as vibrations between the part and the tool, being determined by factors such as discontinuous cutting and inhomogeneity of the blank material etc.;
- rigidity of the technological system, *r*: consists of the tool, part, device and equipment:

$$r = \frac{F}{\delta}, \tag{1}$$

where F represents the cutting force component, and δ is the deformation measured in the force direction;

- the processed part as a source of errors: an important source of errors that involves the dimensions and shape of the parts to be processed;
- cutting temperature: defines the amount of heat that is transferred to the technological system and includes thermal deformations as defects;
- the fixing device of the part: the parts to be processed are clamped in the fixtures by various mechanisms;
- geometrical accuracy of machine tools: during the machining process, machine tools experience

deformations because they are subjected to variable stresses.

Processing errors are classified into three main groups [1,2]:

a) systematic errors (δ_s) - are described by certain laws and are divided into: constant systematic errors ($\delta_s = ct$); variable systematic errors ($\delta_s = k \cdot x$); periodically variable systematic errors $\delta_s = F(t)$. Systematic errors are determined by the use of tools with deviations in shape and size (countersinks, broaches, drills etc.) and from assembly defects in machine tools (deviations in perpendicularity and parallelism of axes), etc.;

b) coincidence errors (random errors) - these occur because their values cannot be predicted, but also because of the large number of actions of independent factors; the occurrence of these errors is variable and multiple;

c) accidental (gross) errors - radically change the results and exceed the admissible limits; they are caused by the operator and are subjective.

2. ASPECTS REGARDING THE PRECISION OF MECHANICAL PROCESSING

The precision of mechanical processing is divided into: dimensional, geometrical, macrogeometrical, and microgeometrical precision.

Microgeometrical precision (roughness) is the set of surface irregularities resulting from the manufacturing process. It can take the form of: material tearing, cracks, striations, pores, gaps, and more. It is influenced by factors such as: cutting regime; tool geometry; properties of the processed material; tool wear; coolant [4,5].

Roughness is determined using one or more parameters. These are, Figure 1 [4,6]:

- R_a - standard deviation of the profile;
- R_z - height of profile irregularities measured at 10 points;
- R_y - maximum profile height;
- S_m - average pitch of irregularities;
- S - average pitch of the local prominences of the profile;
- l - measuring length.

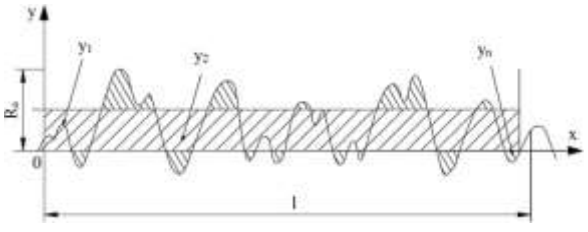

Fig. 1. *Graphical representation of the arithmetic deviation of the profile* [2]

During the manufacturing process, the products that are made are characterized from a mechanical, geometrical etc. point of view by quantities that have generic names of quality characteristics. These characteristics can take different values and depend on the manufacturing process, due to random factors.

In the field of mathematical statistics, these characteristics are called random variables and with their help, various phenomena in the fields of manufacturing and quality are studied.

The *BAC* (*Material-ratio profile*) is a curve that represents the material profile ratio [7]. On the abscissa of the graph in Figure 2, the values of mr (the ratio between material and length) are represented, and on the ordinate, the values of the section are represented.

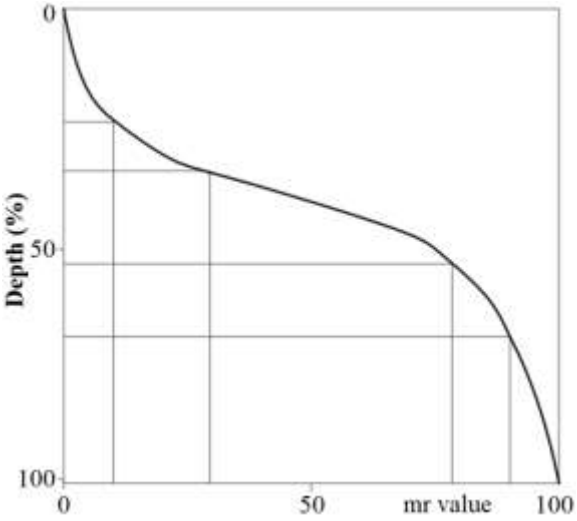

Fig. 2. *BAC graph* [7]

The *ADC* (*Amplitude Distribution Curve*), shown in Figure 3a, is graphically represented using the depth of the first level of the section as the ordinate, and the amplitude density, shown in Figure 3b, for that level of the section as the abscissa [7].

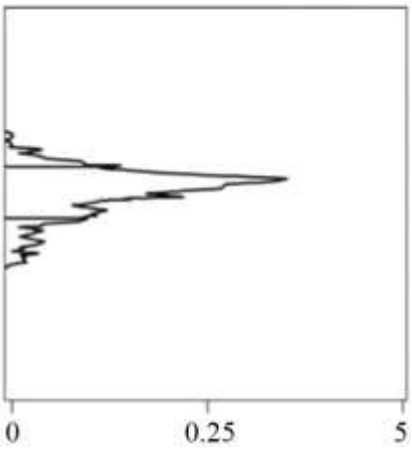

a.

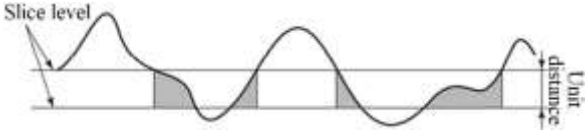

b.

Fig. 3. *Amplitude density (a) and ADC graph (b)* [7]

3. EXPERIMENTAL RESEARCH REGARDING THE MEASUREMENT OF THE SURFACES ROUGHNESS OF THE HYDRAULIC DISTRIBUTOR PART

3.1. Experimental research

In the experiments, three faces of a part called a hydraulic distributor were processed. The factors associated with the quality criteria in the machining process of the part are presented in Figure 4.

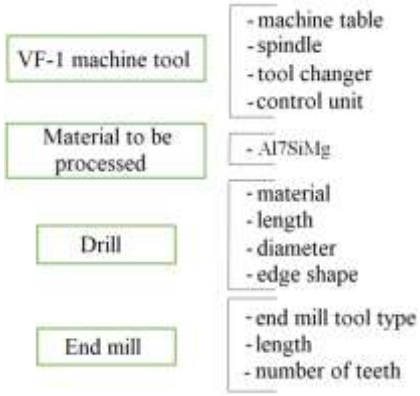

Fig. 4. *Factors associated with quality criteria in the processing of the distributor part*

Also, the schematic representation of the experimental research is given in Figure 5.

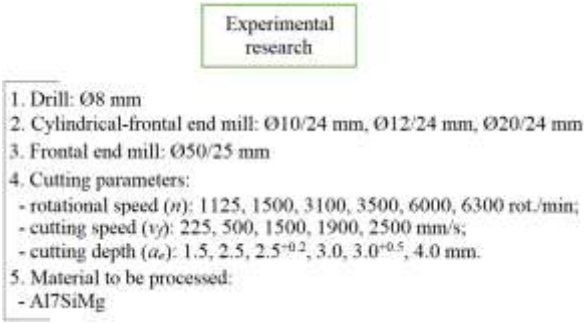

Fig. 5. *Schematic representation of experimental research*

The hydraulic distributor is made of a material called Al7SiMg. It has good processed properties/machinability and excellent corrosion resistance. Processing aluminum alloys is a technological process that is often used [8-10].

The quality of the processed surface serves as an indicator that can provide information about both the machining process that took place and the material properties of the blank.

Silicon-containing aluminum alloys are often used in various applications, such as in foundries and the automotive industry etc. [8,9].

3.2. The equipment and the methodology used in the experimental research

In the experimental research, a drill tool type N/120° - HSSE (5% Ca) with a diameter of Ø8 mm was used, along with three cylindrical-frontal end mills of type N/90° with diameters Ø10/24 mm, Ø12/24 mm, Ø20/24 mm, as well as a frontal end mill tool with a 90° removable plate - APKT 1604-K300 carbide, with a diameter of Ø50/25 mm.

The hydraulic distributor part was processed on a numerically controlled machining center, HAAS brand, VF-1 model [11], located at the Faculty of Engineering, "Dunărea de Jos" University of Galați, Figure 6.

Fig. 6. *CNC equipment, HAAS brand, VF-1 model*

In the experiments, three faces of the part were processed. The processed areas on the three faces are presented in Figure 7.

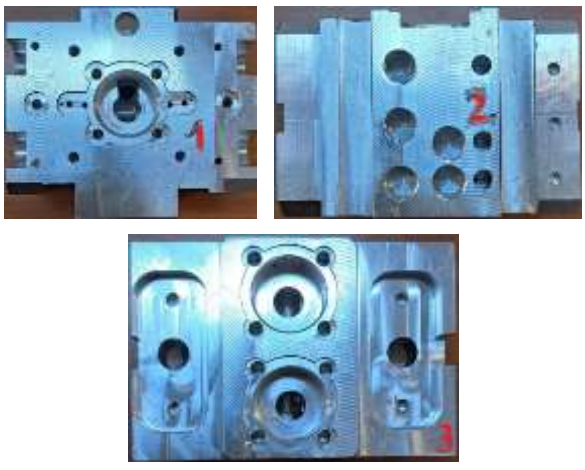

Fig. 7. *The faces of the distributor part*

For face number 1, three operations were performed, noted in Figure 8 as follows:

- *A* - the drilling operation was performed with dimensions Ø8/H3.5 mm, using a drill;
- *B* - is a bore with dimensions $Ø20^{+0.05}$/H12 mm; it was created through a milling operation, with a cylindrical-frontal end mill tool;

- *C* - is a flat surface with dimensions L82/B69 mm; plain milling was performed using a frontal end mill tool.

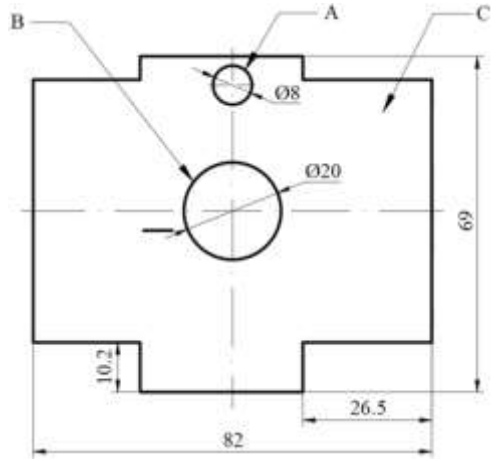

Fig. 8. *Representation of face number 1 of the part*

Table 1 shows the values for each operation processed for face 1: rotational speed, cutting speed and cutting depth.

Table 1. *Cutting parameters for face 1*

Name of the cutting parameters	A	B	C
Rotational speed, *n* [rot/min]	1500	6000	3500
Cutting speed, v_f [mm/s]	500	1500	2500
Cutting depth, a_e [mm]	4.0	$3^{+0.5}$	1.5

For face 2, two operations were performed, presented in Figure 9 as follows:
- *A* - is a linear channel with dimensions L54/B10/H3 mm, made by linear milling using a cylindrical-frontal end mill tool;
- *B* - is a flat surface with dimensions L54/B12 mm; a cylindrical milling was performed, with a cylindrical-frontal end mill tool.

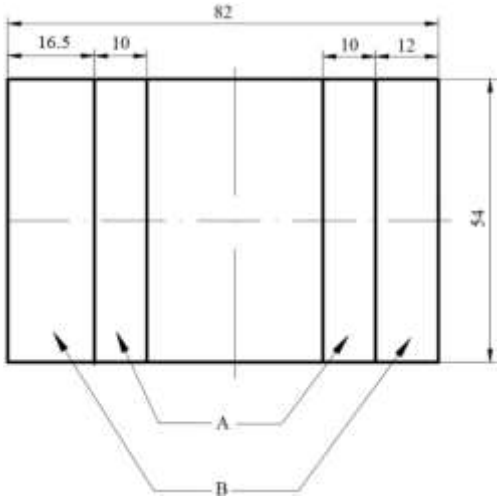

Fig. 9. *Representation of face number 2 of the part*

Table 2 shows the values for each operation processed for face 2: rotational speed, cutting speed and cutting depth.

Table 2. *Cutting parameters for face 2*

Name of the cutting parameters	A	B
Rotational speed, *n* [rot/min]	6300	3100
Cutting speed, v_f [mm/s]	1500	1900
Cutting depth, a_e [mm]	3.0	$2.5^{+0.2}$

For face number 3, four operations were performed, noted in Figure 10 as follows:
- *A* - is a bore with dimensions Ø18/H10 mm; a cylindrical-frontal milling was performed using a cylindrical-frontal end mill tool;
- *B* - is a cavity with dimensions L40/B18/H12/R6 mm; a cylindrical-frontal milling was performed with a cylindrical-frontal end mill tool;
- *C* - is a hole with dimensions Ø8/H5 mm; it was created with a helical drill;
- *D* - is a linear contour with dimensions L54/H5 mm; a cylindrical-frontal milling was performed with a cylindrical-frontal end mill tool.

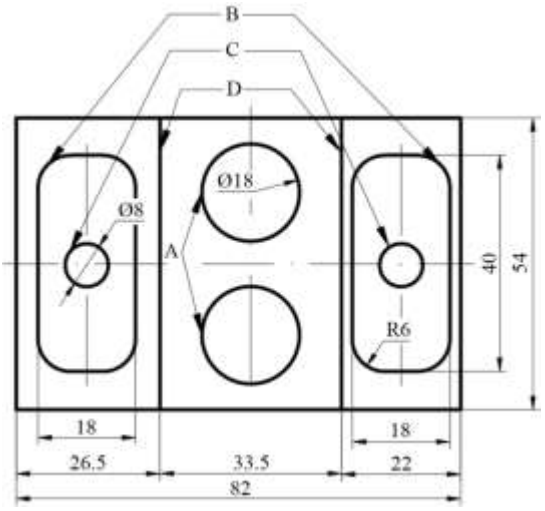

Fig. 10. *Representation of face number 3 of the part*

Table 3 shows the values for each operation processed for face 3: rotational speed, cutting speed and cutting depth.

Table 3. *Cutting parameters for face 3*

Name of the cutting parameters	A	B	C	D
Rotational speed, *n* [rot/min]	6300	6300	1124	3100
Cutting speed, v_f [mm/s]	1500	1500	225	1900
Cutting depth, a_e [mm]	3.0	3.0	4.0	2.5

For the experimental research, a set of roughness measurements (R_a) was performed on the three faces of the part.

For each face, several surfaces were chosen and measured using the Surtronic SJ-210 Mitutoyo equipment, available at the Faculty of Engineering, "Dunărea de Jos" University of Galati.

The roughness measurement is carried out using a palpator that measures a 5 mm portion of the surface of the part and then transmits the obtained result to the screen, as shown in Figure 11.

Fig. 11. *Mitutoyo SJ-210 roughness tester and the palpator*

The roughness measurements taken using the Mitutoyo SJ-210 equipment are as follows:
- for face 1: for surface *B*, 4 measurements were made on the cylinder generator; for surface *C*, 5 measurements were made in the longitudinal direction and 5 measurements in the cross direction;
- for face 2: for surface *A*, 5 measurements were made on the frontal surface and 5 measurements on the cylindrical surface; for surface *B*, 5 measurements were made;
- for face 3: for surface *A*, 3 measurements were made, 5 measurements for surface *B* and 10 measurements for surface *D*.

The steps for measuring with the SJ-210 are:
- the probe was fixed on the surface of the part, and it was checked if the red color on the screen turned blue;
- the file where the first set of measurements will be saved was selected using the buttons: *Enter - Measured data - Enter - folder01 - Blue* key - *Enter*;
- to perform the measurement, the *Start* / *Stop* button is pressed; during the measurement with the palpator, the graph is displayed on the SJ-210 screen, then the roughness value appears;
- to save the value, the *Power* / *Data* key was pressed;
- for the next set of measurements, another file was chosen and the same steps were repeated;
- to check the measured data that has been saved, press *Enter - Measured data - Read*.

4. THE OBTAINED RESULTS

After measuring the roughness (R_a), the following parameters are obtained: R_q (maximum profile height), R_z (profile irregularity height), and the profile evaluation graph.

Table 4 presents the R_a values measured for face 1 of the distributor part, with the graphical representation being presented in Figures 12-17.

Table 4. *R_a values measured for face 1*

Surface B			**Surface C - longitudinal**		
R_a [µm]	**R_q [µm]**	**R_z [µm]**	**R_a [µm]**	**R_q [µm]**	**R_z [µm]**
0.424	0.587	3.516	0.253	0.316	1.614
0.369	0.479	2.656	0.361	0.476	2.688
0.439	0.538	2.691	0.271	0.350	1.957
0.411	0.553	3.240	0.249	0.327	1.910
-	-	-	0.227	0.929	1.556

Surface C - cross		
R_a [µm]	**R_q [µm]**	**R_z [µm]**
0.984	1.174	4.486
0.848	0.964	3.712
0.622	0.719	2.661
0.534	0.625	2.539
0.259	0.308	1.577

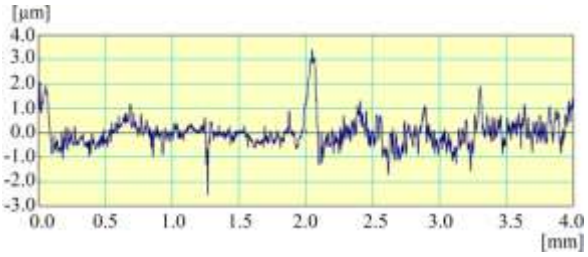

Fig. 12. *Profile evaluation for R_a = 0.424 µm*

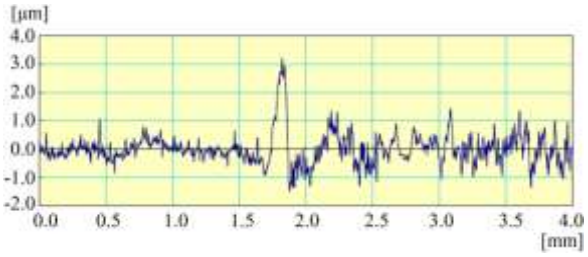

Fig. 13. *Profile evaluation for R_a = 0.369 µm*

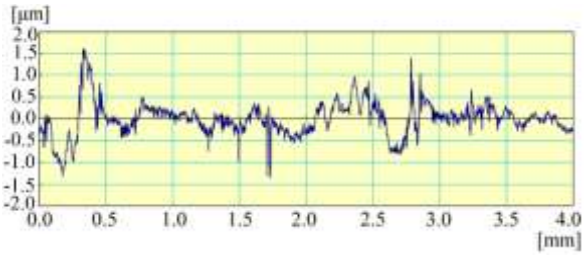

Fig. 14. *Profile evaluation for R_a = 0.271 µm*

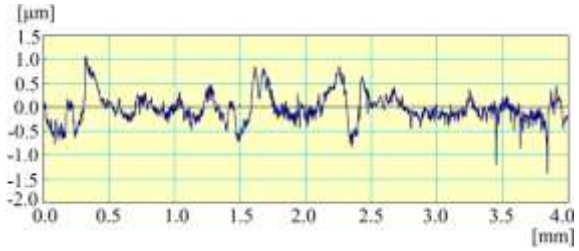

Fig. 15. *Profile evaluation for R_a = 0.227 µm*

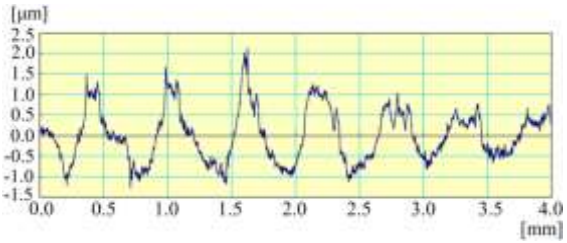

Fig. 16. *Profile evaluation for R_a = 0.534 µm*

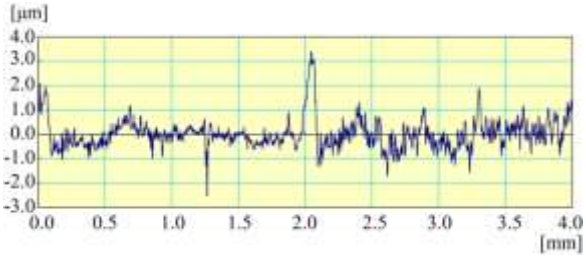

Fig. 17. *Profile evaluation for R_a = 0.259 µm*

Table 5 presents the R_a values measured for face 2 of the distributor part, with the graphical representation being presented in Figures 18-24.

Table 5. *R_a values measured for face 2*

Surface A - frontal			**Surface A - cylindrical**		
R_a [µm]	**R_q [µm]**	**R_z [µm]**	**R_a [µm]**	**R_q [µm]**	**R_z [µm]**
0.870	1.038	4.216	0.201	0.250	1.330
0.896	1.032	4.240	0.240	0.315	1.834
0.929	1.032	3.673	0.211	0.261	1.302
0.940	1.038	3.962	0.224	0.294	1.753
0.749	0.867	3.652	0.178	0.231	1.386
Surface B					
R_a [µm]	**R_q [µm]**	**R_z [µm]**			
0.801	0.801	0.932			
0.737	0.817	2.950			
0.351	0.429	2.253			
0.310	0.392	2.122			
0.423	0.488	1.927			

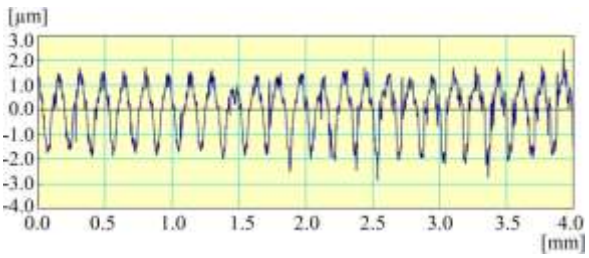

Fig. 18. *Profile evaluation for R_a = 0.870 µm*

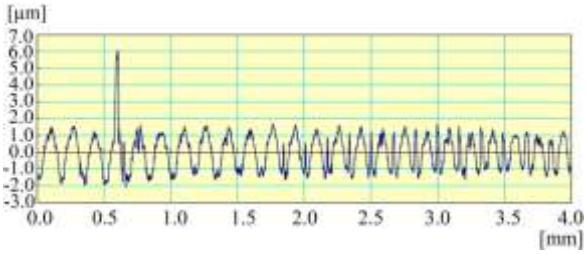

Fig. 19. *Profile evaluation for R_a = 0.896 µm*

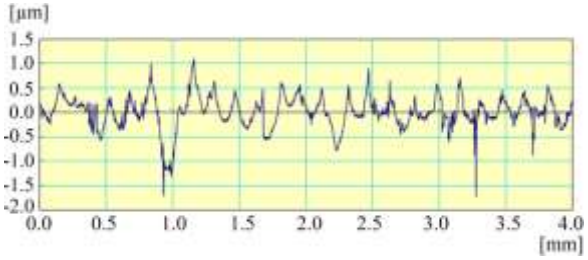

Fig. 20. *Profile evaluation for R_a = 0.240 µm*

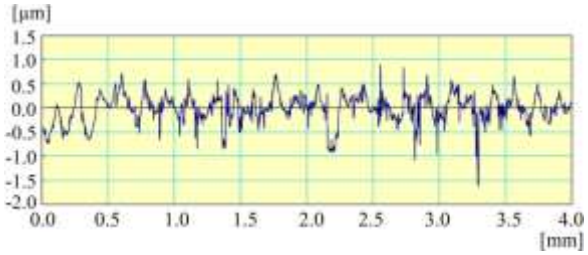

Fig. 21. *Profile evaluation for R_a = 0.224µm*

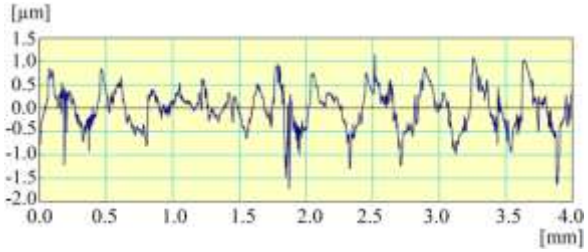

Fig. 22. *Profile evaluation for R_a = 0.351 µm*

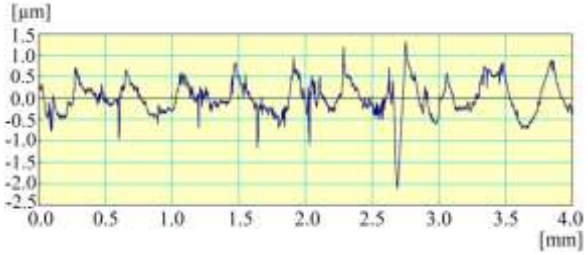

Fig. 23. *Profile evaluation for R_a = 0.310 µm*

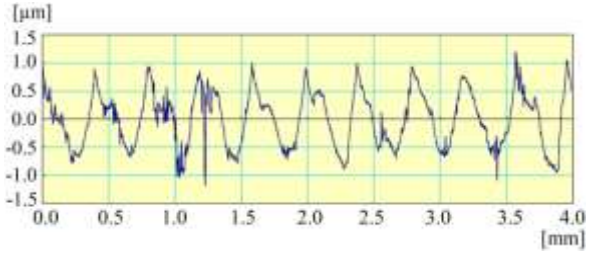

Fig. 24. *Profile evaluation for R_a = 0.423 µm*

Table 6 presents the R_a values measured for face 3 of the distributor part, with the graphical representation being presented in Figures 25-32.

Table 6. *R_a values measured for face 3*

Surface A			Surface B		
R_a [µm]	**R_q [µm]**	**R_z [µm]**	**R_a [µm]**	**R_q [µm]**	**R_z [µm]**
0.478	0.617	3.296	0.670	0.826	4.081
0.475	0.585	3.059	0.758	0.939	4.264
0.582	0.748	4.498	0.864	1.306	6.283
-	-	-	0.623	0.790	3.697
-	-	-	0.558	0.697	3.340
Surface D - right			**Surface D - left**		
R_a [µm]	**R_q [µm]**	**R_z [µm]**	**R_a [µm]**	**R_q [µm]**	**R_z [µm]**
0.757	0.963	4.733	0.444	0.551	2.785
0.592	0.680	2.161	0.505	0.641	2.708
0.486	0.577	2.366	0.433	0.531	2.301
0.522	0.617	2.521	0.494	0.618	2.666
0.472	0.573	2.565	0.462	0.571	2.604

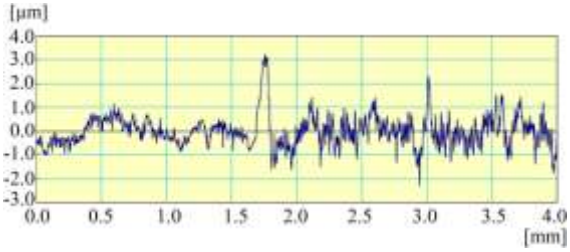

Fig. 25. *Profile evaluation for R_a = 0.478 µm*

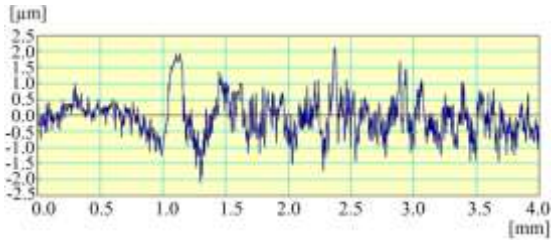

Fig. 26. *Profile evaluation for R_a = 0.475 µm*

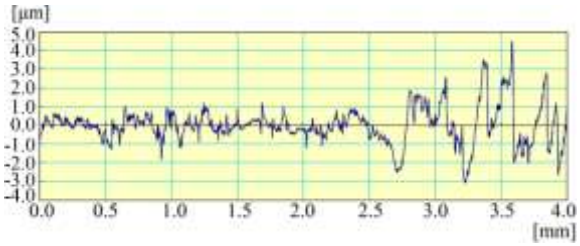

Fig. 27. *Profile evaluation for R_a = 0.670 µm*

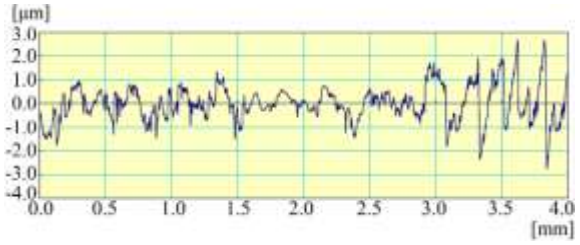

Fig. 28. *Profile evaluation for R_a = 0.558 µm*

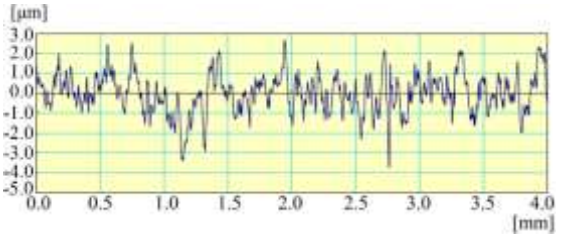

Fig. 29. *Profile evaluation for R_a = 0.757 µm*

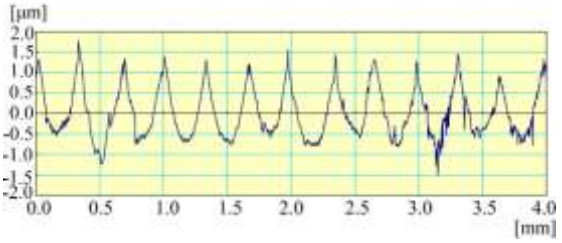

Fig. 30. *Profile evaluation for R_a = 0.522 µm*

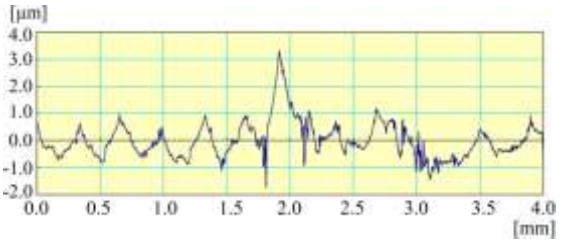

Fig. 31. *Profile evaluation for R_a = 0.494 µm*

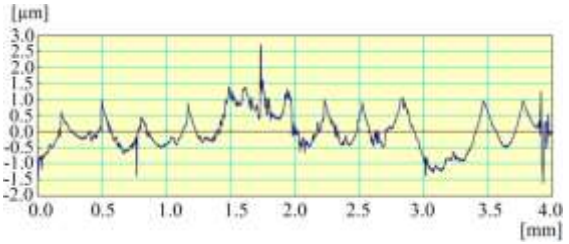

Fig. 32. *Profile evaluation for R_a = 0.462 µm*

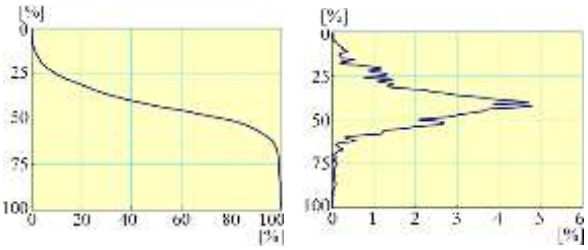

a. *b.*

Fig. 33. *BAC (a) and ADC (b) graphs for R_a= 0.249 µm - face 1*

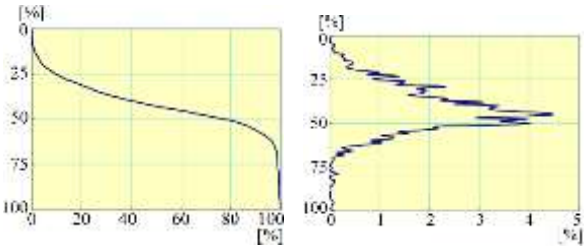

a. *b.*

Fig. 34. *BAC (a) and ADC (b) graphs for R_a = 0.178 µm - face 2*

Also, in Figures 33-36, the *BAC* and *ADC* graphs related to the roughness measured on the 3 faces of the distributor part are presented.

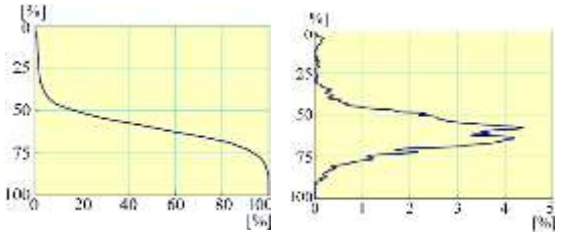

a. *b.*

Fig. 35. *BAC (a) and ADC (b) graphs for R_a = 0.478 µm - face 3*

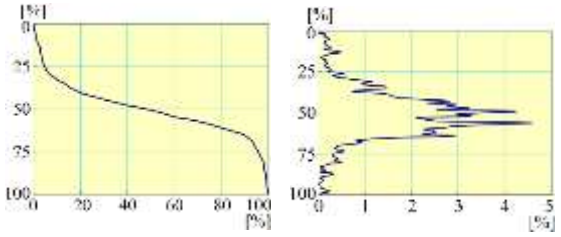

a. *b.*

Fig. 36. *BAC (a) and ADC (b) graphs for R_a = 0.505 µm - face 3*

The *BAC* graphs show good homogeneity of the material profile at low values of R_a roughness, suggesting precise and uniform processing.

Also, the *ADC* graphs demonstrate a concentration of amplitudes within a limited range, indicating effective control of cutting parameters, which minimizes large deviations in microgeometry.

5. CONCLUSIONS

In conclusion, the microgeometry of processed surfaces reflects deviations from the ideal geometry, and their quality is influenced by the traces left by the edges of the tools used. In the case of drilling, milling and boring, surface roughness is determined by factors such as cutting conditions, tool wear, tool material, as well as the use or lack of coolant.

The analysis of the hydraulic distributor part, made of Al7SiMg alloy (a material appreciated for its strength and frequent use in industrial applications), provided important information about the relationship between processing parameters and surface quality. The histogram of R_a values for the three faces of the part is shown in Figure 37.

For face 1, the R_a roughness values on surface *C* in the longitudinal direction are the lowest (0.253 µm), indicating smoother processing in this area.

In the case of face 2, surface *A* (cylindrical) shows the lowest roughness (0.178 µm), demonstrating the efficiency of the cylindrical-frontal end mill tool in achieving smooth surfaces.

In the case of face 3, surface *D* (left) has the lowest R_a value (0.433 µm), being nevertheless higher compared to the other analyzed faces.

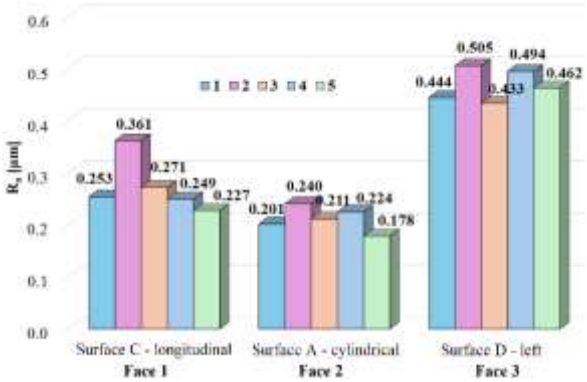

Fig. 37. *Histogram of R_a values [µm]*

From these observations, it can be concluded that the *A* - cylindrical surface on face 2 recorded the lowest R_a roughness values overall.

This highlights the optimal combination of the tool used and the processing regime in order to achieve a superior microgeometry.

The histogram of the results clearly shows the differences between the surfaces, providing a basis for evaluating the influence of processing factors on the quality of the obtained surfaces.

REFERENCES

[1] Gheorghe, D., Georgescu, C., Baroiu, N., *Toleranţe şi control dimensional (Tolerances and dimensional control)*, Ed. Scorpion, Galaţi, ISBN 973-85803-0-7, 2002;

[2] Tarău I., Georgescu C., Otrocol D., *Precizia şi calitatea la prelucrarea materialelor (Precision and quality in material processing)*, Ed. Scorpion, Galaţi, ISBN 973-85803-2-3, 2002;

[3] Lokesh, K.S., Pinto, T., Ramachandra, C.G., *Effect of tool wear & machinability studies on polymer composites: a review*, International Journal of Scientific Research in Mechanical and Materials Engineering, 1(5):71-77, 2017;

[4] Baroiu, N., Costin, G.A., Teodor, V.G., Nedelcu, D., Tăbăcaru, V., *Prediction of surface roughness in drilling ofpolymers using a geometrical model and artificial neural networks*, Materiale Plastice (Plastic Materials), 57(3): 160-173, 2020;

[5] Radu, S.A., *Tehnologii de fabricaţie I (Manufacturing technologies I)*, Ed. U.T. Press, Cluj-Napoca, ISBN 978-606-737-368-4, 2019;

[6] Moroşanu, G.A., Ilie, M., Teodor, V.G., Păunoiu, V., Baroiu, N., *Control of deviations from circularity when drilling polymeric materials*, The Annals of "Dunărea de Jos" University of Galaţi, Fascicle V, Technologies in machine building, ISSN 2668-4829 (Print), 2668-4888 (Online), 41: 59-66, 2023;

[7] GARDCO, *Surftest surface roughness tester*, shttps://www.gardco.com/Products/Surface-Profile-Testers/Surftest-Surface-Roughness-Testers/c/p-64432;

[8] Strihavkova, E., *Analysis of effect of calcium content on machinability of alloys type AlSi7Mg0.3*, 18th International Scientific Conference Engineering for Rural Development, 22-24.05.2019 Jelgava, Latvia, DOI: 10.22616/ERDev2019.18.N222, 2019;

[9] ASRO, *SR EN 1706:2000: Aluminiu şi aliaje de aluminiu. Piese turnate. Compoziţie chimică şi caracteristici mecanice (Aluminium and aluminium alloys. Castings. Chemical composition and mechanical properties)*, https://magazin.asro.ro/ro/standard/25893;

[10] Chavan, S.Y., Jadhav V.S., *Determination of optimum cutting parameters for multiperformance characteristics in CNC and milling of Al-Si7Mg aluminum alloy*, International Journal of Engineering and Technical Research (IJETR), 1(6):15-21, 2013;

[11] Haas F1 Team, Official Machine Tool, *2023 Mill Operator's Manual, Features and functions of a Mill CNC machine,* https://www.haascnc.com/content/dam/haascnc/en/service/manual/operator/english_mill_interactive_manual_print_version_2023.pdf.